

A hypersaline microbial mat from the Pacific Atoll Kiritimati: insights into composition and carbon fixation using biomarker analyses and a ^{13}C -labeling approach

S. I. BÜHRING,^{1,2*} R. H. SMITTENBERG,^{1,3*} D. SACHSE,^{1,4*} J. S. LIPP,² S. GOLUBIC,⁵
J. P. SACHS,^{1,6*} K.-U. HINRICHS² AND R. E. SUMMONS¹

¹Department of Earth, Atmospheric and Planetary Sciences, Massachusetts Institute of Technology, Cambridge, MA, USA

²MARUM – Center for Marine Environmental Sciences, University of Bremen, Bremen, Germany

³Geological Institute, ETH, Zurich, Switzerland

⁴Leibniz Center for Surface Process and Climate Studies, University of Potsdam, Potsdam, Germany

⁵Biology Department, Boston University, Boston, MA, USA

⁶School of Oceanography, University of Washington, Seattle, WA, USA

ABSTRACT

Modern microbial mats are widely recognized as useful analogs for the study of biogeochemical processes relevant to paleoenvironmental reconstruction in the Precambrian. We combined microscopic observations and investigations of biomarker composition to investigate community structure and function in the upper layers of a thick phototrophic microbial mat system from a hypersaline lake on Kiritimati (Christmas Island) in the Northern Line Islands, Republic of Kiribati. In particular, an exploratory incubation experiment with ^{13}C -labeled bicarbonate was conducted to pinpoint biomarkers from organisms actively fixing carbon. A high relative abundance of the cyanobacterial taxa *Aphanocapsa* and *Aphanothece* was revealed by microscopic observation, and cyanobacterial fatty acids and hydrocarbons showed ^{13}C -uptake in the labeling experiment. Microscopic observations also revealed purple sulfur bacteria (PSB) in the deeper layers. A cyclic $\text{C}_{19:0}$ fatty acid and farnesol were attributed to this group that was also actively fixing carbon. Background isotopic values indicate Calvin–Benson cycle-based autotrophy for *cycC*_{19:0} and farnesol-producing PSBs. Biomarkers from sulfate-reducing bacteria (SRB) in the top layer of the mat and their ^{13}C -uptake patterns indicated a close coupling between SRBs and cyanobacteria. Archaeol, possibly from methanogens, was detected in all layers and was especially abundant near the surface where it contained substantial amounts of ^{13}C -label. Intact glycosidic tetraether lipids detected in the deepest layer indicated other archaea. Large amounts of ornithine and betaine bearing intact polar lipids could be an indicator of a phosphate-limited ecosystem, where organisms that are able to substitute these for phospholipids may have a competitive advantage.

Received 29 October 2008; accepted 22 February 2009

Corresponding author: S. I. Bühring. Tel.: +49 421 21865744; fax: +49 421 21865715; e-mail: solveig.buehring@uni-bremen.de

INTRODUCTION

Modern cyanobacterial mats are prevalent in diverse environments including desert crusts, coastal lagoons, hot springs and aquatic hypersaline settings (e.g. Potts, 1994; Jahnke *et al.*, 2001; Jonkers *et al.*, 2003; Wieland *et al.*, 2003). Extreme environmental conditions suppress the activity of grazing organisms (e.g. Cornee *et al.*, 1992;

Fenchel, 1998a) and enable development of mats that may reach gigantic proportions taking the minute scale of their main contributors, cyanobacteria, into account. Phototrophic microbial mats are characterized by daily fluctuations in redox status due to the physiology of the cyanobacteria and associated microorganisms (Canfield *et al.*, 2005). Diatoms are prevalent in the surface layers of many modern mats, possibly because they are well adapted to high irradiance during the day. Oxygen supersaturation is common within and above mats during daytime because

*Present addresses

of high rates of photosynthesis (Jørgensen *et al.*, 1983). At nights, oxygen demand from cyanobacterial respiration and heterotrophy often results in anoxia (Fenchel, 1998b). Anoxygenic phototrophs have been found at the oxygen–sulfide interface under certain light conditions (Pinckney & Paerl, 1997). Sulfate reduction is usually prevalent supplying sulfide for sulfide-oxidizers above (Canfield & Des Marais, 1991). Deeper in the mat, cyanobacterial cell density decreases substantially and oxidation of sulfide and ammonia from underlying sediment dominates (Canfield *et al.*, 2005).

Cyanobacteria are widely considered the first oxygen-producing phototrophs on Earth and are responsible for oxygenating the atmosphere and oceans (e.g. Fischer, 1965; Holland, 2006). They represent a large fraction of marine primary production today (Lochte & Turley, 1988), and most likely since they evolved some 3.5 Ga (Summons *et al.*, 1999; Schopf, 2006; Knoll *et al.*, 2007). The timing of the inception of oxygenic photosynthesis is both uncertain and controversial. However, there is evidence in the form of stromatolites that complex microbial communities, possibly including cyanobacteria, existed in shallow seas as early as 3.5 Ga (Allwood *et al.*, 2006; Altermann *et al.*, 2006) and that, by the Neoarchean (2.7–2.5 Ga), they were principal builders of wide carbonate platforms (Knoll, 2003). Living microbial mats can therefore be useful as modern analogs for early stromatolites to examine ancient processes such as their potential role in the production of reduced gases on early Earth (Hoehler *et al.*, 2001), quantification of oxygen and carbon cycling with respect to salinity (Canfield *et al.*, 2004) or the role of anoxygenic phototrophs on calcification (Bosak *et al.*, 2007).

Lipid analyses of microbial communities (e.g. Rajendran *et al.*, 1992; Rütters *et al.*, 2002a) and their fossil counterparts (e.g. Summons *et al.*, 1996) offer valuable insights into microbiological diversity. The Archaean sedimentary record suffers from the scarcity of preserved and recognizable microbial remains (Altermann, 2004); so, molecular fossils are a valuable source of information (e.g. Brocks *et al.*, 1999; Brocks & Summons, 2003). The in-depth study of the biomarker structure is therefore necessary to improve recognition of source organisms and interpretation of the early sedimentary record. The information gained from identifying biomarkers and their distributions can be further increased by simultaneous determination of the stable carbon isotope composition of these lipids. Natural abundance studies take advantage of the small difference in isotope ratios found in nature (Peterson, 1999; Hayes, 2001), due to the fact that enzyme-catalyzed reactions discriminate against ^{13}C . Stable isotopic data can be useful for gaining inferences about ancient biochemistries (e.g. Schidlowski *et al.*, 1983) in identifying trophic relationships and in determining the mode of carbon fixation (e.g. Hayes, 2001).

Additionally, ^{13}C -labeled substrates can be used to decipher carbon flows in microbial systems. In such studies, a portion of the stable isotope tracer is incorporated into the biomass of organisms that actively metabolize the labeled substrate (e.g. Middelburg *et al.*, 2000; van der Meer *et al.*, 2007).

In this study, a hypersaline microbial mat system from a lake on the central Pacific island of Kiritimati was investigated for microscopic structure and lipid biomarkers including their C-isotopic compositions. A simple labeling experiment using ^{13}C -bicarbonate allowed us to identify carbon flow into lipid biomarkers. Our motivation was to characterize carbon fixation and turnover and to pinpoint lipids with potential to be specific for different groups of organisms and their physiologies.

MATERIALS AND METHODS

Kiritimati Island

Kiritimati (01°52' N, 157°20' W) lies within the Northern Line Islands of the Republic of Kiribati (Fig. 1A). It is the largest coral atoll in the world with a surface area of ~360 km². Approximately one-quarter of Kiritimati surface is covered by brackish to hypersaline lakes, some of which connect to a large lagoon in the north-western part of the island (Fig. 1B). The majority of these lakes represent basins of evaporating sea water trapped following a high sea level in the mid-Holocene (Valencia, 1977; Woodroffe & McLean, 1998). Even though Kiritimati experiences a large variability in precipitation (Saenger *et al.*, 2006 and references therein) that can change the lake salinities dramatically over short timescales, the overall climate is evaporative and microbial mats are well developed in many of the islands' lakes. Recharge of the lakes and ponds occurs primarily during El Niño Southern Oscillation (ENSO) events, when torrential rains and higher sea levels can cause flooding.

Environmental setting

Figure 1C and D shows the position and a panorama of Lake 2A on the Island of Kiritimati, covering an area of 0.02 km² and holding a maximum depth of 20 cm. Microbial mats were well laminated (Fig. 1E), easily accessible and had a uniform appearance over a large area. Salinity, pH and dissolved oxygen (DO) were measured using a portable YSI Sonde 6600 connected to an YSI 650 MDS data logger (YSI, Yellow Springs, OH, USA). On the day of sampling, the temperature varied around 30 °C, the pH of the water was 7.9 and the salinity 116. The water was oxygen supersaturated (105% in the morning and 126% in early afternoon); the DO was 3.8 mg L⁻¹ at 09:00 hours and 4.8 mg L⁻¹ at 13:00 hours. The top 5–7 cm comprised the actively growing microbial community

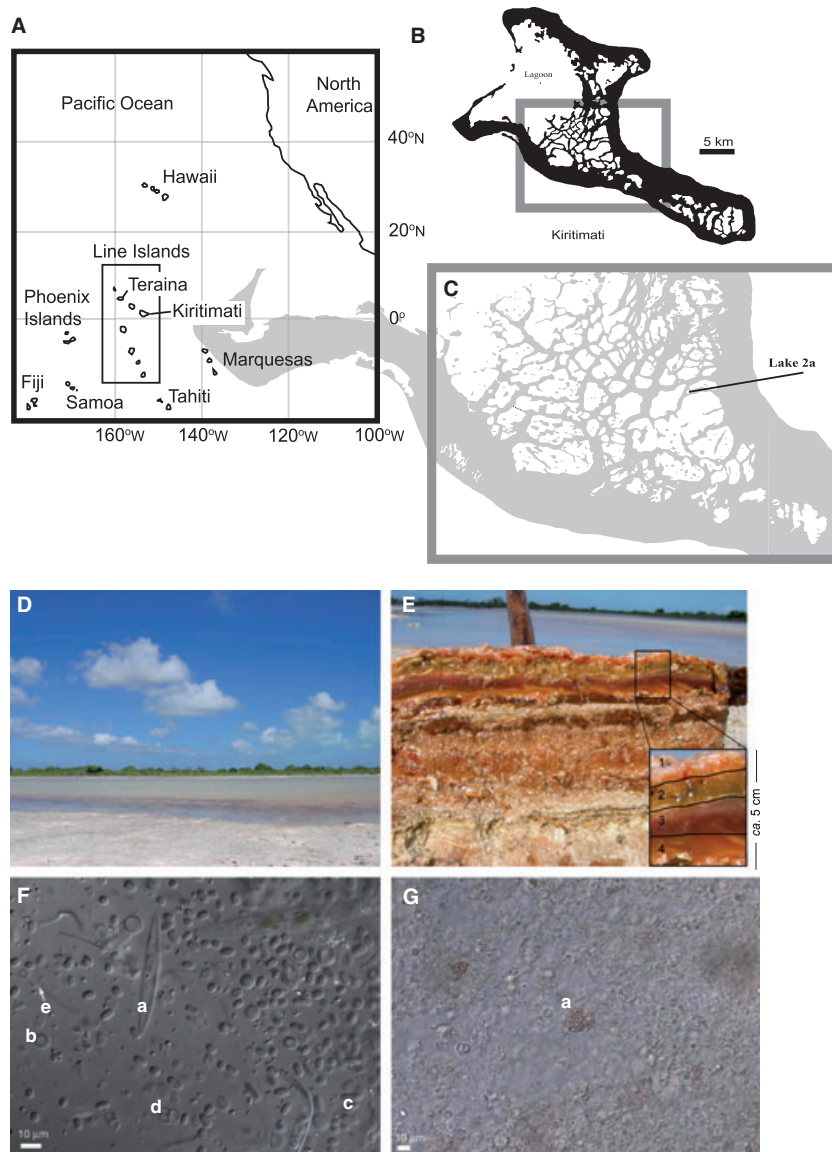


Fig. 1 (A) Geographic position of (B) Kiritimati Island (formerly known as Christmas Island) in the Northern Line Islands, Republic of Kiribati (based on Saenger *et al.*, 2006) with the frame (C) showing the position of the Lake 2A; (D) Lake 2A on Kiritimati Island; (E) Vertical section through the mat with the four investigated layers magnified in the insert; (F) Photomicrograph from the upper gelatinous layer (magnification: 100 \times), a = *Nitzschia*; b = *Aphanocapsa*; c = *Aphanothece*; d = *Entophysalis*; e = sheaths von *Phormidium/Leptolyngbya*; (G) Photomicrograph from the fourth layer (magnification: 63 \times): a = PSB.

(Fig. 1E), underlain by approximately 80 cm of sediment, rich in calcite and halite, above a carbonate hard ground.

Labeling experiment

Representative mat sections, 7 cm deep with an area of approximately 100 cm², were placed in plastic containers of 1 L filled with lake water. Sodium bicarbonate (¹³C: 99%; Cambridge Isotope Laboratories, Inc., Andover, MA, USA) was predissolved in a few milliliters of distilled water and added to the incubations such that the final concentrations reached approximately 200 μ M. Following duplicate labeled incubations of 6-h duration, and a control experiment in which no label was added, the mat edges were excised to exclude the possibility of lateral incorporation and the samples were sectioned into four layers on the

basis of color and consistency. These comprised an upper layer (~5 mm) of orange, fluffy gelatinous organic material with halite crystals, a second layer (~5–15 mm) of denser green/orange biomass, also mixed with halite, a third layer (~15–40 mm) of solid gelatinous, orange-purple biomass and a fourth (~40–60 mm) layer of solid gelatinous yellow/orange material. Distinction between the layers was incomplete because of diffuse boundaries and surface irregularities. Sections were then sealed in plastic bags, frozen and transported to MIT in a cooler. Inspection of samples after arrival showed that these were partially thawed. However, there is no evidence that the lipid distribution was altered by degradation. We also attempted a killed control experiment adding Lugol's solution (I₂/KI) to the overlying water, where considerable label uptake at the end of the experiment revealed that it was unsuccessful. Only layer

1 was used for investigating ^{13}C -uptake into lipid biomarkers, because almost no label was detected in layer 2.

Microscopy

Microscopy was performed with a Zeiss Axioimager A1 microscope (Carl Zeiss GmbH, Göttingen, Germany) and Zeiss AxioCam MRc Imaging system and software. Enumeration was performed at 40 \times magnification. Identification of morphotypes was in accordance with traditional phycological manuals (Geitler, 1932; Komárek & Anagnostidis, 1999, 2005) and Bergey's Manual of Systematic Bacteriology (Castenholz, 2001) as well as by consulting current published work on microbial ecology (Campbell & Golubic, 1985; Garcia-Pichel *et al.*, 1998; Richert *et al.*, 2006).

Lipid extraction, derivatization and detection

Samples were freeze dried prior to extraction, spiked with internal standard (1-*O*-hexadecyl-2-acetyl-*sn*-glycero-3-phosphocholine; PAF), and were extracted ultrasonically using the method for intact polar lipids (IPLs) after Sturt *et al.* (2004). Lipids were further separated on 2-g silica columns (deactivated with 5% water) using 15 mL of hexane, 18 mL of hexane/DCM (2 : 1), 18 mL of DCM/acetone (9 : 1) and 20 mL of methanol to yield hydrocarbons, ketones + esters, alcohols and polar lipids respectively.

The polar lipids were transesterified overnight at 70 °C using 1 mL of acetyl chloride and 9 mL of anhydrous methanol under nitrogen atmosphere. Alcohols were converted to trimethylsilyl (TMS) ether derivatives with 50 μL of BSTFA (bis-trimethylsilyltrifluoroacetamide) and 100 μL of pyridine at 80 °C for 1 h.

Compound quantifications and identifications were performed using Agilent 6890 Series II gas chromatographs (Agilent Technologies Inc., Santa Clara, CA, USA), one equipped with a flame ionization detector (GC-FID) and the other equipped with an Agilent 5973 Mass Selective Detector (Agilent Technologies Inc., Santa Clara, CA, USA) (GC-MSD) operated at 70 eV. Both instruments used programmable temperature vaporization (PTV) inlets, 60-m Varian Chromapak CP-Sil 5 capillary columns (Varian, Inc., Palo Alto, CA, USA) (0.32 mm i.d.; 0.25 μm film thickness) and helium as the carrier gas. For GC-MSD, conditions were as follows: injection at 60 °C while the oven was held at the same temperature for 1 min. Subsequently, the oven temperature was raised to 150 °C (120 °C) at 10 °C min^{-1} (20 °C min^{-1}) followed by a rate of temperature increase of 4 °C min^{-1} to 320 °C, and an 15 (25)-min isothermal period for fatty acids/alcohols (for hydrocarbons). Quantification was conducted using internal standards: nonadecanoic acid, nonadecanol and *n*-hexatriacontane. GC-FID conditions were the same as

for GC-MSD. Identification was performed by comparison of mass spectra with those reported in the literature, while in some cases use was also made of relative retention times, as for *cyt*C_{19:0}.

Isotopic composition of fatty acids, alcohols and hydrocarbons were determined using coupled gas chromatography–combustion–isotope ratio mass spectrometry (GC-C-IRMS). At Woods Hole Oceanographic Institution, an Agilent model 6890 GC equipped with a DB-5 (60 m, 0.32-mm i.d. and 0.25- μm film thickness column) was coupled via a Combustion Interface III to a ThermoFinnigan Delta Plus mass spectrometer (ThermoFisher, Bremen, Germany). At MIT, a similar set-up comprised a ThermoFinnigan Trace GC equipped with a J&W DB-5MS column (60 m \times 0.32 mm, 0.25-mm film) and coupled with a combustion furnace interfaced to a Finnigan MAT DeltaPlus XP isotope ratio monitoring mass spectrometer. Both were operated with ISODAT 2.0 software. Chromatographic conditions were initially 60 °C for 2 min, then 60–320 °C at 6 or 8 °C min^{-1} . Samples were analyzed in duplicates. The accuracy of isotope results was monitored routinely with standards (obtained from A. Schimmelmann, Indiana University) and found to be 0.3‰ or lower. Sample replicates produced standard errors less than 0.5‰ vs. VPDB. Isotope results were corrected for the introduction of the additional carbon atoms during derivatization with acidic methanol or BSTFA (Abrajano *et al.*, 1994). Internal standards for quantification were added prior to extraction.

High-pressure liquid chromatography-mass spectrometry analysis was performed at the University of Bremen using the same settings as described by Sturt *et al.* (2004). Relative concentrations of IPLs were calculated based on MS response of molecular ions relative to that of known amounts of the internal standard. The values of the phosphatidylglycerol diacylglycerol (PG-DAG), phosphatidylethanolamine diacylglycerol (PE-DAG), monoglycosyldiacylglycerol (Gly-DAG), phosphatidylcholine diacylglycerol (PC-DAG) and diglycosyl glyceroldialkylglyceroltetraether (2Gly-GDGT) were corrected for their response factor determined using commercially available standards. Lack of authentic standards for some IPL types prevented determination of the response factor; therefore, we used an average value for typical IPLs.

Bacterioplanepolyols (BHPs) were prepared via acetic hydrolysis with acetic acid in methanol (0.1 vol%) for 1 h at 70 °C and subsequent acetylation and analyses via GC-MS, applying the method of Talbot & Farrimond (2007).

Data analysis

Carbon isotopic ratios ($^{13}\text{C}/^{12}\text{C}$) are expressed in the delta notation ($\delta^{13}\text{C}$) relative to Vienna Pee Dee Belemnite Standard ($^{13}\text{C}/^{12}\text{C}_{\text{VPDB}} = 0.0112372 = R_{\text{VPDB}}$):

$$\delta^{13}\text{C} (\text{‰}) = [(R_{\text{sample}}/R_{\text{std}}) - 1] \times 1000,$$

where R_{sample} and R_{std} are the $^{13}\text{C}/^{12}\text{C}$ of sample and standard (Craig, 1957) respectively. Incorporation as ^{13}C is reflected as excess (above background samples) ^{13}C and is expressed in terms of total uptake (I) as well as specific uptake (i.e. $\Delta\delta^{13}\text{C} = \delta^{13}\text{C}_{\text{sample}} - \delta^{13}\text{C}_{\text{control}}$ after Middelburg *et al.*, 2000). Total uptake I of ^{13}C in lipids was calculated as the product of excess ^{13}C (E) and concentration of the respective compound. E is the difference between the fraction F of the sample and background:

$$E = F_{\text{sample}} - F_{\text{background}},$$

where $F = ^{13}\text{C}/(^{13}\text{C} + ^{12}\text{C}) = R/(R + 1)$ and $R = (\delta^{13}\text{C}/1000 + 1) \times R_{\text{VPDB}}$.

RESULTS

Microscopic observations

Visual impression of the microscopic observations is given in Fig. 1F and G. The microscopic observations are given as abundance scores from 0 to 5 for the different groups in Fig. 2 (0 = not present, 1 = 0–10%, 2 = 10–25%, 3 = 25–50%, 4 = 50–75% and 5 = 75–100%). In the top layer, the cyanobacterium *Aphanocapsa* sp. was the largest contributor in terms of abundances. We also found considerable amounts of *Aphanothece* spp. and the diatom *Nitzschia* sp. Minor amounts of the cyanobacterium *Entophysalis* sp. and the filamentous cyanobacterium *Leptolyngbya* were present, mostly as trichomes inside a distinct sheath. In the second layer, *Entophysalis* and *Aphanocapsa* dominated, followed

by *Aphanothece* and *Leptolyngbya*. In the deeper layers empty sheaths of *Leptolyngbya* were abundant, possibly due to higher resistance to degradation. Microscopically, purple sulfur bacteria (PSB) could only be observed in the third and fourth layers. In the third layer, the PSBs were accompanied by *Aphanocapsa*, whereas, in the fourth layer, besides *Aphanocapsa* and PSBs, filaments of *Leptolyngbya* were also abundant.

Fatty acid composition

Compound compositions of the different layers are given in Table 1 and Fig. 3. The phospholipid-derived fatty acids (PLFAs) were clustered into eight groups (Fig. 3A). In the first layer, 28% of the PLFAs were saturated, followed by 19% for $\text{C}_{16:1\omega7} + \text{C}_{18:1\omega9}$ PLFAs, whereas only 3% can be attributed to *Cyc* $\text{C}_{19:0}$. In the second layer, the saturated fatty acids were the most abundant group (39%), followed by $\text{C}_{16:1\omega7} + \text{C}_{18:1\omega9}$ (16%). *Cyc* $\text{C}_{19:0}$ increased to 7% of the total. In the third and fourth layers, the saturated fatty acids (45% and 38%) were again the most important group of PLFAs. *Cyc* $\text{C}_{19:0}$ gained greater importance in the third

Table 1 Lipid composition of different layers of the microbial mat

Depth interval	Lipid component ($\mu\text{g g}^{-1}$ dry mat)		
	Fatty acids	Alcohols	Hydrocarbons
Layer 1	44×10^3	220	31
Layer 2	35×10^3	140	21
Layer 3	43×10^3	280	24
Layer 4	35×10^3	270	27

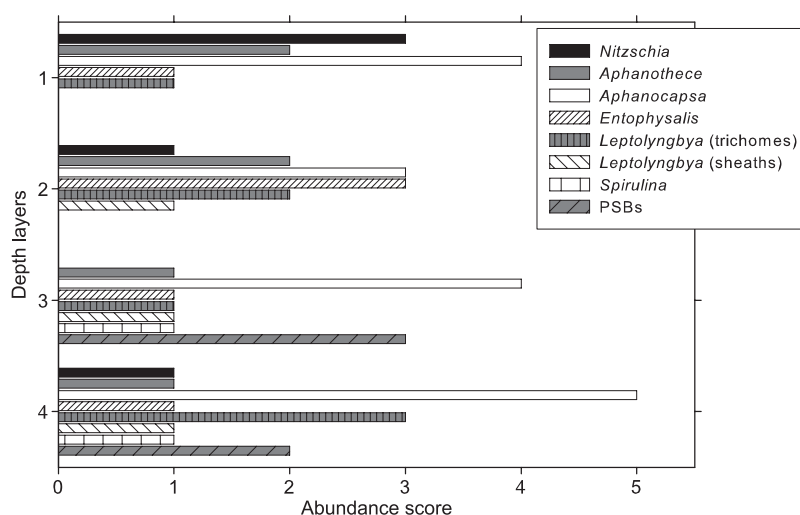


Fig. 2 Relative abundance of microorganisms in the layers of the mat based on microscopic observations, the assessment is given in scores of 1–5 of their relative abundance in % of total biomass (5 = 100–75%, 4 = 75–50%, 3 = 50–25%, 2 = 25–10% and 1 = 10–0.1%, score 1 means that there was at least one specimen found).

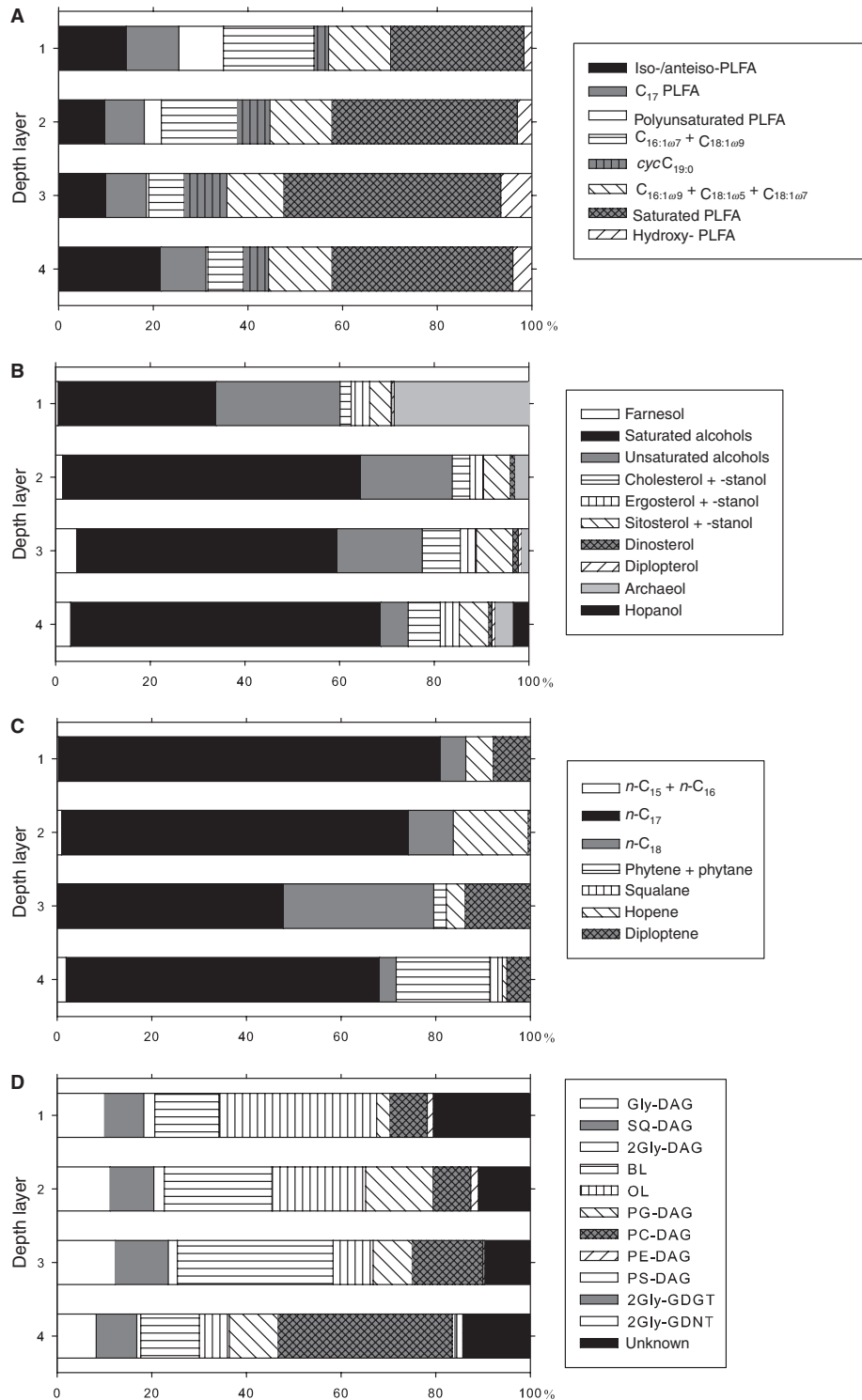


Fig. 3 Lipid biomarker distribution over depth: (A) PLFAs (*iso-/anteiso*-PLFA: *i*C_{14:0}, *i*C_{15:0}, *ai*C_{15:0}, *i*C_{16:0}; C₁₇ PLFA: *cyc*C_{17:0}, *i*C_{17:0}, *ai*C_{17:0}, C_{17:1 ω 8}, C_{17:1 ω 6}, C_{17:0}; polyunsaturated PLFA: C_{16:2} and C_{18:2}; saturated PLFA: C_{14:0}, C_{15:0}, C_{16:0}, C_{18:0}; hydroxy-PLFA: 12-*OH*-C_{19:0}, 14-*OH*-C_{21:0}, 12-*OH*-C_{21:0}); (B) alcohols (saturated alcohols: C_{15:0}-OH, C_{16:0}-OH, C_{17:0}-OH, C_{18:0}-OH, C_{20:0}-OH to C_{28:0}-OH, and C_{30:0}-OH; unsaturated alcohols: C_{17:2}-OH, C_{17:1}-OH, C_{18:1}-OH, C_{20:1}-OH, C_{22:1}-OH); (C) hydrocarbons (*n*-C₁₇: *n*-C_{17:0} and two *n*-C_{17:1} isomers; hopenes: hop-17(21)-ene and hop-21-ene), (D) IPLs (Gly-DAG, monoglycosyldiacylglycerol; SQ-DAG, sulfoquinovosyldiacylglycerol; 2Gly-DAG, diglycosyldiacylglycerol; BL, betaine lipids; OL, ornithine lipids; PG-DAG, phosphatidylglycerol diacylglycerol; PC-DAG, phosphatidylcholine diacylglycerol; PE-DAG, phosphatidylethanolamine diacylglycerol; PS-DAG, phosphatidylserine diacylglycerol; 2Gly-GDGT, glyceroldialkylglyceroltetraether; 2Gly-GDNT, glyceroldialkylnonitoltetraether).

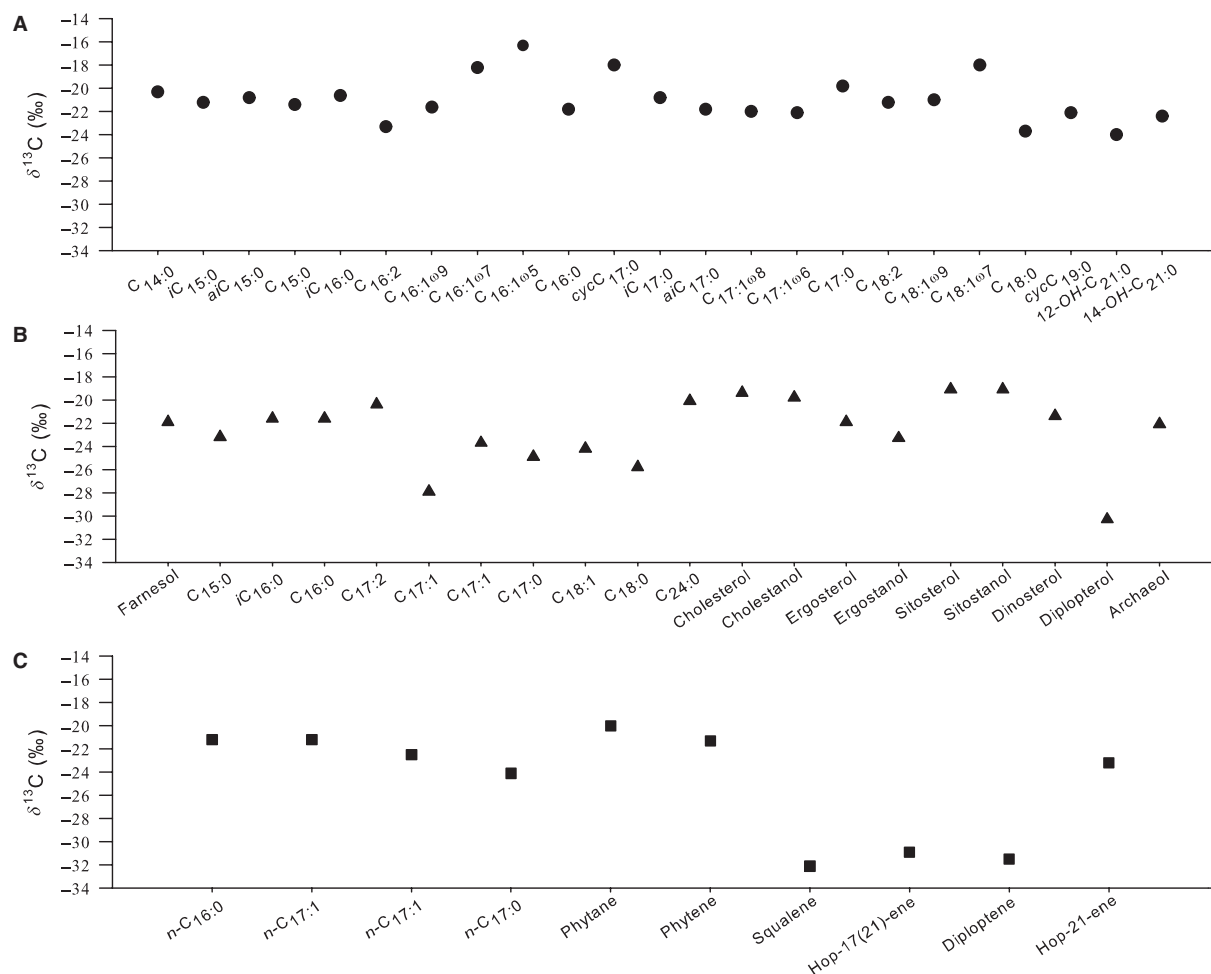


Fig. 4 Stable carbon isotopic composition ($\delta^{13}\text{C}$) of lipids extracted from the first layer of an untreated microbial mat of (A) PLFAs; (B) alcohols; (C) hydrocarbons.

layer, reaching 9% of the fatty acids. In the fourth layer, the *iso-/anteiso*-PLFAs reached 22%.

The natural abundance isotopic compositions ($\delta^{13}\text{C}$) of the fatty acids from the first layer were mainly between -20‰ and -24‰ (Fig. 4A). The fatty acids C_{16:1 ω 7}, cycC_{17:0} and C_{18:1 ω 7} were slightly heavier with values around -18‰ . The heaviest value was detected for C_{16:1 ω 5} (-16.3‰).

Alcohol composition

The distribution of alcohols is displayed in Fig. 3B. In the first layer, the saturated alcohols accounted for 33% of the total alcohols, followed by archaeol (bis-*O*-phytanlylglyceroldiether) with 28% (Fig. 3B). In the deeper layers, saturated alcohols became more prominent, reaching 66% of the alcohols. Different sterols (cholesterol, ergosterol and sitosterol) and their saturated counterparts were found in varying amounts (between 2% and 8%) in each

layer. Farnesol was present in minor amounts in all layers, reaching its maximum with approximately 5% in the third layer.

$\delta^{13}\text{C}$ values of the alcohols in the first layer were between -20‰ and -24‰ for most of the investigated components (Fig. 4B). Some components were more depleted in ^{13}C including one OH-C_{17:1} isomer (-27.9‰), OH-C_{18:0} (-25.8‰) and diplopterol (-30.3‰). Sitosterol and sitostanol were slightly more enriched than the average (-19.1‰ each) and cholesterol and cholestanol had values of -19.4‰ and -19.8‰ respectively.

Hydrocarbon composition

The distribution of hydrocarbons (Fig. 3C) revealed a clear dominance of *n*-C₁₇, comprising up to 80% of total hydrocarbons in the top layer. Similar hydrocarbon distributions have been observed in other microbial mats from Kiritimati (Sachse & Sachs, 2008). *n*-C₁₈ was prominent in the third

layer, reaching 32%. Phytene and phytane were abundant in the deepest layer, comprising 20% of the hydrocarbons. Their isotopic compositions are displayed in Fig. 4C. As with the sterols, the majority of the measured hydrocarbons have $\delta^{13}\text{C}$ values between -20‰ and -24‰ . Lighter values were observed for squalene (-32.1‰), hop-17(21)-ene (-30.9‰) and diploptene (-31.5‰).

Intact polar lipid composition

Intact polar lipid distributions are displayed in Fig. 3D. In the first layer, ornithine lipids (OL) were most abundant, comprising 33% of total IPLs, followed by the betaine lipids (BL) with 14%. The BLs were the most abundant IPLs in the second and third layers (23% and 33% respectively). OLs and PG-DAG were also abundant in the second layer (20% and 14% respectively). Gly-DAG was an abundant component in all layers, contributing 10%, 11%, 12% and 8% from the first to fourth layers respectively. PC-DAG was the major IPL only in the deepest layer (37%). Phosphatidylserine diacylglycerol (PS-DAG) and the archaeal components, 2Gly-GDGT and diglycosyl glyceroldialkylnonitoltetraether (2Gly-GDNT), were only detected in the deepest layer (0.4%, 0.5% and 1.2% respectively). 2Gly-GDGTs occurred with one or zero pentacyclic rings. 2Gly-GDNT was identified via the characteristic loss of one sugar head group and a daughter ion of m/z 1456, indicative of four pentacyclic rings in the biphytane chains.

Bacteriohopanepolyols

We found traces of $17\beta(H)$, $21\beta(H)$ -bacteriohopanetetrol (BHT) in the third layer. In all four layers, traces of $17\beta(H)$, $21\beta(H)$ -32-hopanoic acid were found, whereas $17\beta(H)$, $21\beta(H)$ -30-hopanol and $17\beta(H)$, $21\beta(H)$ -33-hopanoic acid could only be detected in the third and fourth layers.

^{13}C -labeling experiment

The results of the C-isotopic labeling experiment suggested an active photosynthetic carbon-fixing community. Label uptake was apparently confined to the surface layers as we found only a minor uptake in the second and no isotopic enrichment in layers 3–4. Dissolved inorganic carbon (DIC) isotopic composition in the overlying water was not determined. However, as the lake was shallow and well mixed, equilibrium with atmospheric CO_2 can be assumed, i.e. a DI^{13}C value close to 1‰ , similar to that of the Pacific (Takahashi *et al.*, 2000).

Fatty acids

Uptake of the labeled ^{13}C -bicarbonate showed remarkable differences for the different PLFAs (Fig. 5A and B). The specific uptake was the highest in $\text{C}_{14:0}$, $\text{C}_{16:0}$ and $\text{C}_{18:0}$, as

indicated by the high $\Delta\delta^{13}\text{C}$ values of these PLFAs: 28‰, 17‰ and 15‰ respectively (Fig. 5A). The total uptake accounts for the concentration of each analyte. The highest total uptake was detected for $\text{C}_{16:0}$, reaching values as high as $1.0 \mu\text{g }^{13}\text{C g}^{-1}$ dry mat. Considerable uptake also took place in $\text{C}_{18:1\omega7}$ and $\text{C}_{18:0}$, with mean values around $0.2 \mu\text{g }^{13}\text{C g}^{-1}$ dry mat. The total uptake into all fatty acids for the two replicates were $3.2 \mu\text{g }^{13}\text{C}$ and $1.2 \mu\text{g }^{13}\text{C g}^{-1}$ dry mat.

Alcohols

The specific uptake was the highest for $\text{C}_{15:0}\text{-OH}$ (72‰) and $\text{C}_{17:0}\text{-OH}$ (35‰) (Fig. 6A). The total incorporation into alcohols was generally lower than into PLFAs (Fig. 6B) because of their generally lower concentrations. The highest uptake was associated with $\text{C}_{15:0}\text{-OH}$ and archaeol with 1.0 and $0.6 \times 10^{-3} \mu\text{g }^{13}\text{C g}^{-1}$ dry mat respectively. In the two parallel incubations, the total uptake into alcohols was 6.1 and $4.5 \times 10^{-3} \mu\text{g }^{13}\text{C g}^{-1}$ dry mat respectively.

Hydrocarbons

High specific uptake was measured for diploptene (13‰), followed by one $n\text{-C}_{17:1}$ isomer (10‰), $n\text{-C}_{16:0}$ (8‰) and hop-17(21)-ene (7.5‰) (Fig. 7A). The highest total uptake was determined for $n\text{-C}_{17:0}$, with a mean value of $0.8 \times 10^{-3} \mu\text{g }^{13}\text{C g}^{-1}$ dry mat (Fig. 7B). Diploptene was also characterized by a high total uptake, reaching $0.4 \times 10^{-3} \mu\text{g }^{13}\text{C g}^{-1}$ dry mat (Fig. 7B). The values for the total uptake in all hydrocarbons were 1.9 and $0.8 \times 10^{-3} \mu\text{g }^{13}\text{C g}^{-1}$ dry mat for the two replicate incubations.

DISCUSSION

This study of a hypersaline microbial mat from Kiritimati was designed in order to characterize the biomarkers with potential to identify active microbial groups and physiologies using a combination of microscopic investigations together with biomarker characterization including labeling techniques. The layers of the mat revealed considerable differences, regarding the microscopically determined microbial distribution and the biomarker structure. Biomarkers could be assigned to different organisms, comparing our microscopic investigations with the biomarker abundances and isotopic compositions. Our interpretation of the ^{13}C -labeling experiment is summarized in Fig. 8, revealing that an uptake over the 6-h course of the experiment was not confined to photoautotrophs, but also involved re-mineralization of the newly fixed carbon by organotrophic bacteria and incorporation by archaea.

Microscopic observations revealed the dominance of cyanobacteria in this hypersaline mat system (Fig. 2). The top layer was dominated by intact cells of *Aphanocapsa* and

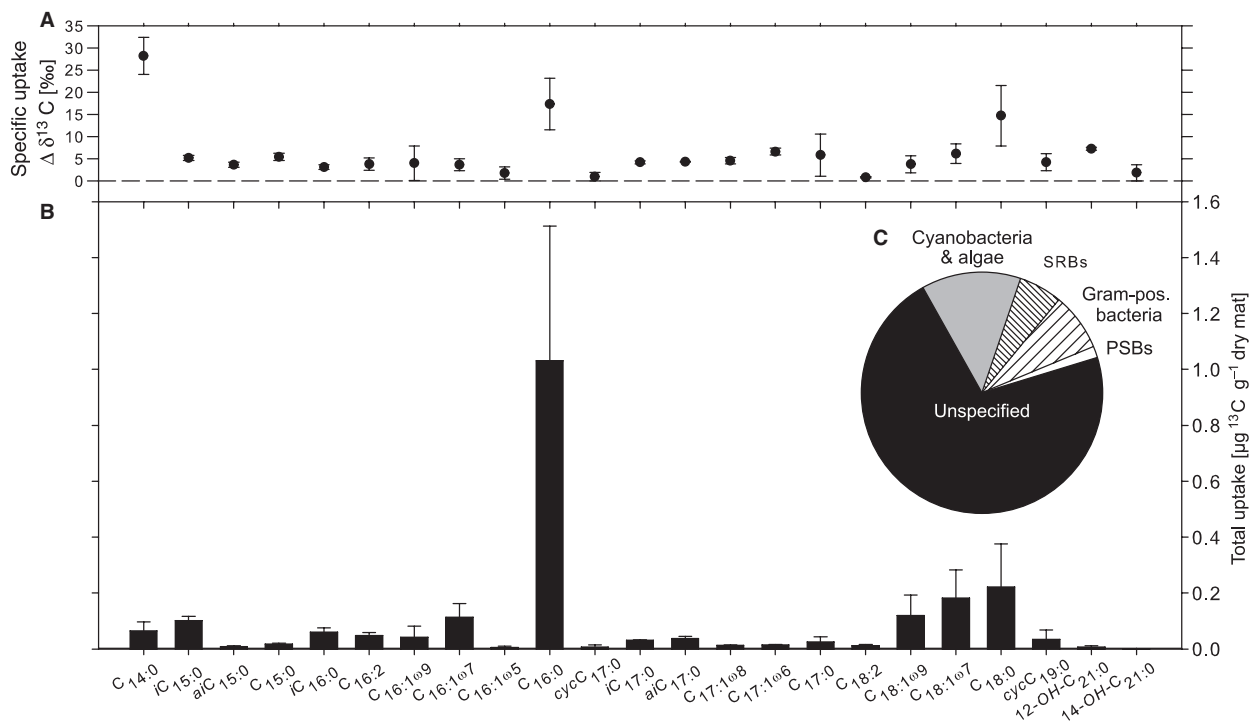


Fig. 5 (A) Specific uptake ($\Delta\delta^{13}\text{C}$) into PLFAs of the first layer; (B) total uptake into PLFAs of the first layer; (C) total uptake into grouped PLFAs [cyanobacteria + algae: polyunsaturated PLFAs and $\text{C}_{16:1\omega7} + \text{C}_{18:1\omega9}$; sulfate-reducing bacteria (SRBs): C_{17} PLFAs; Gram-positive: branched saturated PLFAs; purple sulfur bacteria (PSBs): $\text{cycC}_{19:0}$] after 6 h of incubation. Error bars indicate range of two replicate incubations.

Aphanothece spp., suggesting a vital cyanobacterial community. Species of these genera are often described as the principle contributors to hypersaline microbial mat systems at numerous localities (e.g. Javor, 2002). The terminology describing these coccoid halophilic morphotypes in the literature is not consistent; they are sometimes used interchangeably or named *Synechococcus*, *Cyanothece* and *Halothece* (see Garcia-Pichel *et al.*, 1998). In addition to cyanobacteria, the diatom *Nitzschia* was abundant in the surface layer. Diatoms are known to contribute regularly to the top layers of microbial mats (e.g. Mir *et al.*, 1991).

Based on fatty acids alone it can be difficult to discriminate between cyanobacteria and algae, especially because no long-chain polyunsaturated PLFA (PUFA) could be detected in our samples, which would be a clear indicator for diatoms. We attributed the C_{16} and C_{18} PUFA (e.g. Dunstan *et al.*, 1994), the fatty acids $\text{C}_{16:1\omega7} + \text{C}_{18:1\omega9}$ and the C_{17} hydrocarbons to the group cyanobacteria and algae (Fig. 8). We viewed $\text{C}_{16:1\omega7} + \text{C}_{18:1\omega9}$ primarily as cyanobacterial markers (Caudales *et al.*, 2000; Gugger *et al.*, 2002; de Oteyza *et al.*, 2004) based on the fact that cyanobacteria were the most abundant group in the mat and that these fatty acids occurred in all layers, decreasing in abundance with depth (Fig. 3A). The labeling experiment also revealed considerable uptake into PLFAs attributed to cyanobacteria, accounting for at least 13% of the

^{13}C incorporation into PLFAs (Fig. 5C). This is a potential underestimation, as the ubiquitous $\text{C}_{16:0}$ is prevalent in cyanobacteria (e.g. Kenyon *et al.*, 1972). The cyanobacterial hydrocarbons $n\text{-C}_{17:0}$ and $n\text{-C}_{17:1}$ (Chuecas & Riley, 1969; Grimalt *et al.*, 1991) accounted for up to 80% of the total hydrocarbons (Fig. 3C), consistent with the importance of cyanobacteria in this mat system. The rapid ^{13}C uptake into C_{17} hydrocarbons and diploptene (Fig. 7) is in accordance with this interpretation. Phytene and phytane were important components in the third and fourth layers of the mat (Fig. 3C). They are diagenetic products and probably derived from the phytol side chain of chlorophyll or bacteriochlorophyll (Bchl) (Volkman & Maxwell, 1986). Diplopterol was present in layers of all depths in our mat, its abundance increased with depth (Fig. 3B). Diplopterol can be attributed to a variety of bacteria including cyanobacteria (Rohmer *et al.*, 1984), PSB (Ourisson *et al.*, 1987), methylotrophs (Summons *et al.*, 1994) and *Desulfovibrio* (Blumenberg *et al.*, 2006). The labeling experiment revealed no label uptake into this compound (Fig. 6), which makes a phototrophic source in our setting unlikely. Noteworthy is a considerable uptake of ^{13}C into diploptene (Fig. 7), indicating a different biological source for this compound than for diplopterol. Other studies also revealed that in some bacterial strains diploptene was present but not diplopterol (Joyeux *et al.*, 2004; Härtner *et al.*, 2005).

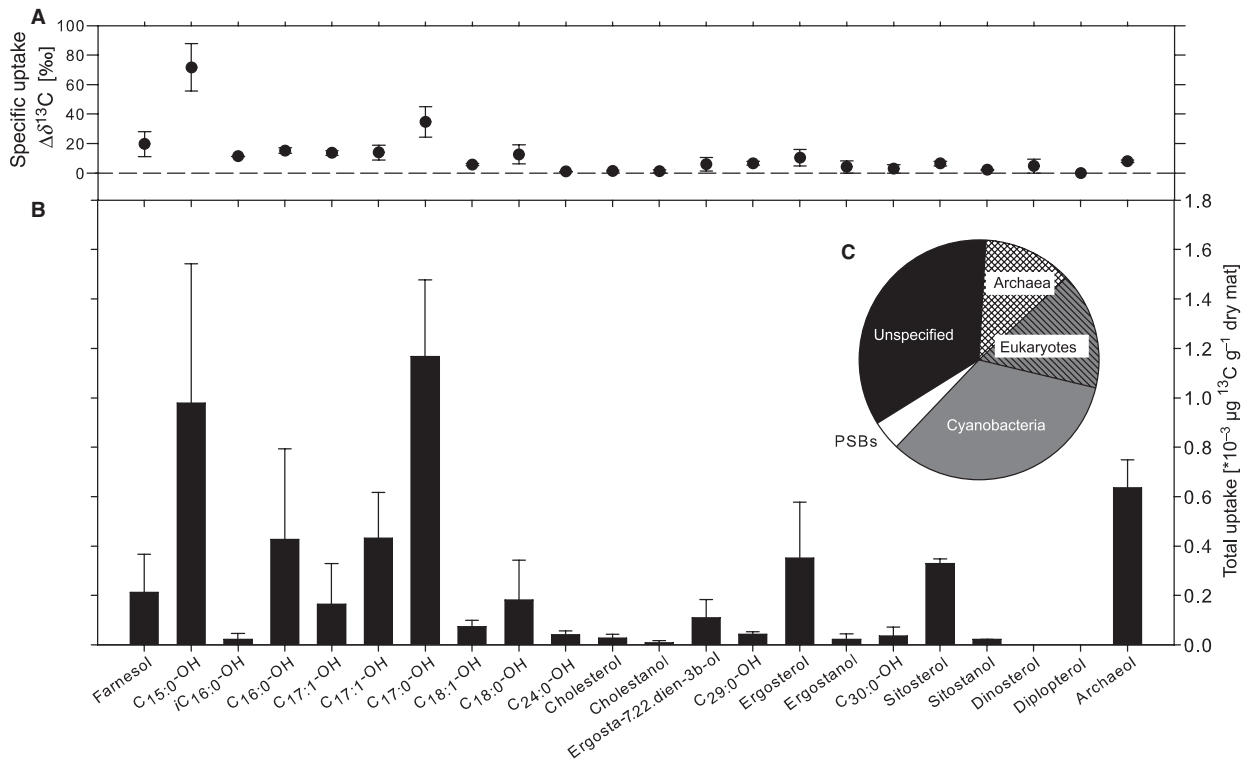


Fig. 6 (A) Specific uptake ($\Delta\delta^{13}\text{C}$) into alcohols of the first layer; (B) total uptake into alcohols of the first layer after 6 h of incubation; (C) total uptake into grouped alcohols (archaea: archaeol; eukaryotes: ergosterol + ergostanol, sitosterol + sitostanol; cyanobacteria: C₁₇-ols; purple sulfur bacteria (PSBs): farnesol) after 6 h of incubation. Error bars indicate range of two replicate incubations.

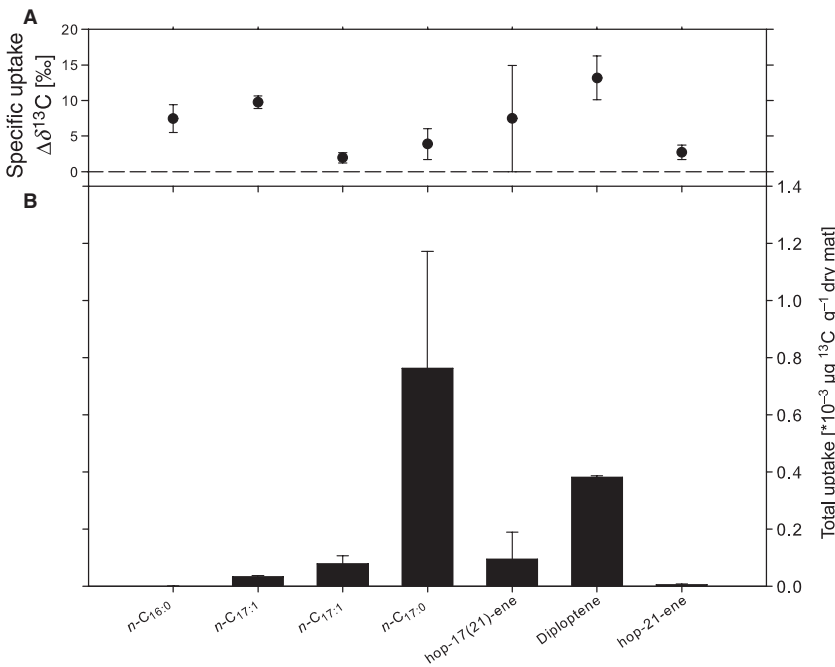


Fig. 7 (A) Specific uptake ($\Delta\delta^{13}\text{C}$) into hydrocarbons of the first layer; (B) total uptake into hydrocarbons of the first layer after 6 h of incubation. Error bars indicate range of two replicate incubations.

Cyanobacteria are known to be one of the most prolific sources of BHPs (Talbot *et al.*, 2008). Traces of BHT were detected in the third layer of the mat, where *Aphanocapsa*

was the dominating cyanobacterium (Fig. 2). BHT has been detected in different members of the Chroococcales and in other cyanobacterial mats (Talbot *et al.*, 2008) but is also

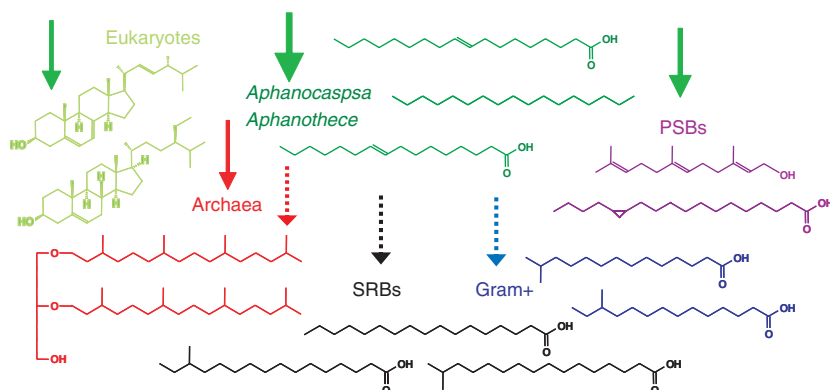


Fig. 8 Working model for the carbon flow under light conditions in the hypersaline microbial mat, solid arrows represent autotrophy (green: photoautotrophy, red: chemoautotrophy), whereas dashed lines represent heterotrophy.

widespread in the bacterial domain (e.g. Rosa-Putra *et al.*, 2001; Blumenberg *et al.*, 2006) and often found in sedimentary environments (e.g. Talbot & Farrimond, 2007). Cholesterol is a general marker for eukaryotes (Volkman, 1986) and may therefore derive from diatoms in the Kiritimati mats, notwithstanding their minimal uptake of ^{13}C -label at the time of the experiment (Fig. 6).

The common cyanobacterial and chloroplast IPLs, Gly-DAG, 2Gly-DAG, SQ-DAG and PG-DAG (Kiseleva *et al.*, 1999; Okazaki *et al.*, 2006), were abundant in this mat. Ritter & Yopp (1993) found Gly-DAG, 2Gly-DAG and PG-DAG in *Aphanothece halophytica* but not SQ-DAG. In addition to these IPLs, BLs are abundant in the thylacoid membranes of eukaryotic algae (Dembitsky, 1996). PC-DAG, PE-DAG and PS-DAG are generally not found in cyanobacteria (Wada & Murata, 1998).

The second important group of phototrophs in this system are the anoxygenic phototrophs, which are probably mainly represented by PSB. Typical biomarkers for PSB are *cycC*_{19:0} and farnesol (Fig. 8), even though we cannot exclude a different source in our setting, because our biomarker data do not match the microscopic observation. The *cycC*_{19:0} fatty acid occurs abundantly in the lipids of PSB, such as *Ectothiorhodospira* (Grimalt *et al.*, 1991). The relative abundances of this PLFA increased slightly with depth, peaking in the third layer (Fig. 3A). Further, its $\delta^{13}\text{C}$ value of -22.1‰ is consistent with autotrophic carbon fixation via the Calvin–Benson cycle. From the labeling experiment, we calculated a contribution of 1% to total carbon fixation for *cycC*_{19:0} fatty acid in the first layer (Fig. 5C). This small contribution to carbon fixation in the first layer matches the microscopic data that revealed no detectable PSBs at this level and their known preference for low-light environments and low oxygen tension (e.g. Hirschler-Rea *et al.*, 2003). The alcohol fraction contained farnesol, the primary ester-bound alcohol side chain of Bchl e, d and g (Airs *et al.*, 2001) and C_{16:0}-OH, another

Bchl side chain (Glaeser & Overmann, 2003). These Bchls are the photosynthetic pigment of both PSB (Hirschler-Rea *et al.*, 2003) and purple non-sulfur bacteria, as well as green sulfur bacteria and green non-sulfur bacteria (filamentous anoxygenic phototrophs) (Permentier *et al.*, 2000; Nübel *et al.*, 2002; Glaeser & Overmann, 2003). An origin of farnesol from green sulfur bacteria is unlikely because these organisms use the reverse citric acid cycle, which causes relatively small carbon isotope fractionation resulting in $\delta^{13}\text{C}$ values of approximately -12‰ (e.g. Manske *et al.*, 2005). A $\delta^{13}\text{C}$ value of -21.9‰ for farnesol (Fig. 4B) points to PSB as the most likely source, and ^{13}C -uptake indicates that the PSBs were actively fixing carbon (Fig. 6A). PSBs produce a variety of IPLs, with Gly-DAG, 2Gly-DAG, PC-DAG, PE-DAG and PG-DAG being particularly common (Linscheid *et al.*, 1997), all were present in our mat. Purple non-sulfur bacteria and several other Gram-negative bacteria accumulate BLs and OLs (Imhoff *et al.*, 1982) under phosphate-limiting conditions (Benning *et al.*, 1995). Abundant OLs suggest that phosphate may therefore have been limiting mat growth in Lake 2A (Fig. 3D).

Sulfate-reducing bacteria are prevalent in microbial mats and their activity is tightly coupled with cyanobacterial carbon fixation (Canfield & Des Marais, 1991). They also promote lithification and may be instrumental for mat preservation in the geological record (reviewed by Baumgartner *et al.*, 2006). C₁₇ PLFAs are typical constituents of SRBs (Boschker & Middelburg, 2002; Fig. 8), which were present at all depths (Fig. 3A). The uptake into C₁₇ fatty acids in the first layer of the mat accounted for 6% of the total uptake into PLFAs (Fig. 5). The relatively high ^{13}C -uptake suggests a close coupling between SRBs and phototrophs (Fig. 8), as also reported by other authors (e.g. Frund & Cohen, 1992; Decho *et al.*, 2005). The close coupling is possible only if SRBs can tolerate oxygen exposure (e.g. Postgate, 1959), a phenomenon demonstrated by

Cypionka *et al.* (1985). Krekeler *et al.* (1998) reported different oxygen-escaping strategies for SRBs in microbial mats, like migration to anoxic zones, formation of clumps and oxygen removal by active respiration in bands. They also found 20 times lower most probable number counts of SRBs during the day under oxic conditions than at night. By contrast, Canfield & Des Marais (1991) reported highest rates of sulfate reduction in the oxic zone of a hypersaline mat system from Guerrero Negro, Baja California, Mexico. Our results suggest the presence of an active sulfate-reducing community operating during the day in the upper, generally oxic zone of the microbial mat.

Gram-positive bacteria are abundant in hypersaline environments (Caton *et al.*, 2004; Ghozlan *et al.*, 2006) and stromatolites (Burns *et al.*, 2004). Branched saturated fatty acids (mainly *i*C_{15:0}, *ai*C_{15:0} and *i*C_{16:0} in our setting) are often their primary fatty acids (Lechevalier & Lechevalier, 1988; Romano *et al.*, 2008), even though an origin in SRB cannot be excluded (e.g. Rütters *et al.*, 2002b). The relative abundance of the *iso/anteiso*-group was high in layers of all depths (Fig. 3A), reaching a maximum of approximately 22% in the deepest layer. Eight percent of the total PLFA ¹³C-label uptake occurred into *i*C_{15:0}, *ai*C_{15:0} and *i*C_{16:0} (Fig. 5B), indicating a tightly coupled carbon cycle in the mat (Fig. 8). Different Gram-positive bacteria were investigated for their IPL composition by Schubotz (2005) who found PE-DAG, PG-DAG and diphosphatidylglycerol (DPG) in all isolates. With PE-DAG representing only a minor constituent and DPG being absent in our mat, we cannot exclude a different origin for the branched saturated fatty acids we observed.

Archaea, affiliated with the *Methanosarcinales*, the *Halo-bacteriales* and uncultured *Euryarchaeota*, mainly from the marine benthic group D (MBGD), were detected by Sørensen *et al.* (2005) in a hypersaline mat from Eilat, Israel. Crenarchaeota and euryarchaeota were detected in hypersaline stromatolites by Papineau *et al.* (2005), while Burns *et al.* (2004) also observed methanogenic archaea of the *Methanosarcinales* group in stromatolites.

Archaeol is a biomarker that derives from archaea (Koga *et al.*, 1998). It was detected in all layers and was especially abundant in the top layer (Fig. 3B). In our experiment, it accounted for a considerable label uptake (Figs 6 and 8). Like SRB, methanogenic archaea can be autotrophic in their use of CO₂ and H₂ (Hoehler *et al.*, 2001) and this could explain the observed ¹³C-uptake into both groups. Another possible origin of the labeled archaeol could be methanogens taking up non-competitive substrates, like trimethylamines (TMA), formerly produced by carbon-fixing cyanobacteria (King, 1988; Orphan *et al.*, 2008). A vital community of methylotrophic methanogens would also be supported by our observation that archaeol concentrations were maximal in the top layer of the mat. Uptake of TMA would be accompanied by a stoichiometric uptake

of CO₂ (e.g. Londry *et al.*, 2008). Bearing in mind that the DIC in the upper layers of the mat would comprise ¹³C-enriched carbon diffusing down from the water column and some ¹³C-depleted carbon derived from respiration, the measured δ¹³C of archaeol (−22‰) and its enrichment in the labeling experiment would be compatible with a primary origin from methylotrophic methanogens (Summons *et al.*, 1998; Londry *et al.*, 2008). Alternatively, heterotrophic halophilic archaea could have assimilated cyanobacterial exudates in the sunlit surface layer (Burns *et al.*, 2004).

We also detected intact tetraether lipids that derive from archaea (Sturt *et al.*, 2004) in the deepest layer. Jahnke *et al.* (2008) found archaea even dominating above bacteria in the deeper layers of a hypersaline microbial mat of Baja California. GDGTs occur in a variety of archaea (e.g. Hopmans *et al.*, 2000; Sinninghe Damste *et al.*, 2002; Sturt *et al.*, 2004) in several environments, including the deep biosphere (Biddle *et al.*, 2006; Lipp *et al.*, 2008). GDNTs were so far only attributed to the hyperthermophile crenarchaeon *Sulfolobales* (Hanford & Peeples, 2002; Sturt *et al.*, 2004), which is an unlikely source in our setting. Biddle *et al.* (2006) and Lipp *et al.* (2008) found GDNT in the deep biosphere, which is an additional indicator suggesting a more widespread occurrence of this compound, maybe indicating an organism related to the sulfur cycle (suggested by Sturt *et al.*, 2004).

Non-phosphatidyl polar lipids accounted for 44–75% of total IPLs in different layers of our mat (Fig. 3d). Van Mooy *et al.* (2006) found membrane lipids devoid of P accounting for over 90% of IPLs in picocyanobacteria in the North Pacific tropical gyre and hypothesized that substitution of S for P in membrane lipids could offer a competitive advantage for organisms living in phosphate-limited environments. Besides abundant Gly-DAG, 2Gly-DAG and SQ-DAG, we also found other non-phosphatidyl lipids including BLs and OLs. BLs are abundant in many eukarya, including algae, bryophytes, fungi and some protozoa (Dembitsky, 1996). These lipids have also been discovered in the photosynthetic purple bacterium *Rhodospira sphaeroides* (Benning *et al.*, 1995). They resemble the more commonly known PC-DAG in molecular geometry and charge distribution, and probably substitute this substance in membranes under phosphate-limiting growth conditions (Araki *et al.*, 1991). As the physiological importance of non-phosphatidyl polar lipids is currently not understood, it is also possible that the high content is an adaptation to environmental factors, like high salinity.

Lipids that derive from the amino acid ornithine are widespread among bacteria (Lopez-Lara *et al.*, 2003), especially in the Gram-negative bacteria (Ratledge & Wilkinson, 1988) but have not been found in eukarya or archaea. These lipids are also described as being produced in some bacteria under phosphorus-limiting conditions

(Benning *et al.*, 1995; Weissenmayer *et al.*, 2002; Choma & Komaniecka, 2003). Aygun-Sunar *et al.* (2006) showed that OLs are required for maintaining optimal steady-state amounts of some extracytoplasmic proteins, important for various cellular processes, including electron transport.

The sterol ratio $C_{27-29\Delta 0}/C_{27-29\Delta 5}$ increased from 0.2 for the top three layers to 0.5 in the deepest layer. This is in agreement with a sterol production only in the upper layers of the mat becoming gradually buried by upward growth of the phototrophic community. Longer exposure to the increasingly reducing conditions promotes diagenetic alterations of the sterols. However, uptake of the label into several stanols may also be consistent with these lipids having a functional role in the mat community.

CONCLUSIONS

Based on microscopic and organic-geochemical analyses, cyanobacteria (*Aphanocapsa* and *Aphanothece*) were found to dominate the hypersaline mat system on Kiritimati, represented by different fatty acids and hydrocarbons with considerable label uptake. Anoxygenic phototrophs were represented by the fatty acid *cyc* $C_{19:0}$ and the alcohol farnesol, with an isotopic composition revealing carbon fixation via the Calvin–Benson cycle. Label uptake by SRBs indicated close coupling with carbon-fixing organisms. Archaeol was detected and found to be responsible for considerable label uptake after 6 h of incubation, indicating active archaea in the top layer of the mat. Our approach combining lipid analyses with a simple labeling experiment and microscopic investigations of a recent microbial mat successfully revealed that different prokaryotic groups prosper in close proximity and mutual dependence. Many of the groups that we found are of great geobiological relevance, because they are thought to be the main constructors of analog ancient microbial mat systems (Allwood *et al.*, 2006; Altermann *et al.*, 2006). Our results may aid in tracing microbial evolution in the geological record, but more lipid biomarker-based mat studies are needed to get a representative overview of the diversity in modern systems.

ACKNOWLEDGEMENTS

We are grateful to C. Saenger and M. Miller for their help in the field and K. Anderson, J. Bryden and S. Fukada for logistical support. Thanks are due to S. Sylva for his kind collaboration. C. Colanero and C. Harms are acknowledged for their help with the laboratory work. M. Elvert and F. Schubotz are acknowledged for their assistance with mass spectral interpretation. The insightful comments by the reviewers and the subject editor, Christopher House, are gratefully acknowledged. Thanks are due to the Republic of Kiribati for allowing access to the lake. The field work was funded by the MIT Earth System Initiative

Exploration Fund Award and a Gary Comer Abrupt Climate Change Foundation award to JPS, who was additionally funded by the US National Science Foundation (NSF-ESH-0639640). SIB was funded by a Marie Curie Outgoing International Fellowship (MOIF-CT-2004-509865) from the European Community and a MARUM postdoctoral Fellowship, DS was funded by a Feodor-Lynen Research Fellowship of the Alexander von Humboldt Foundation, Bad Godesberg, Germany, JSL by the Deutsche Forschungsgemeinschaft (Grant Hi 616/4-2) and SG by the Alexander von Humboldt Foundation. RES was supported by the Hanse Wissenschaftskolleg, the Alexander von Humboldt Foundation and the NASA Astrobiology Institute during the preparation of this report.

REFERENCES

- Abrajano TA Jr, Murphy DE, Fang J, Comet P, Brooks JM (1994) $^{13}C/^{12}C$ ratios in individual fatty acids of marine mytilids with and without bacterial symbionts. *Organic Geochemistry* **21**, 611–617.
- Airs RL, Borrego CM, Garcia-Gil J, Keely BJ (2001) Identification of the bacteriochlorophyll homologues of *Chlorobium phaeobacteroides* strain UdG6053 grown at low light intensity. *Photosynthesis Research* **70**, 221–230.
- Allwood AC, Walter MR, Kamber BS, Marshall CP, Burch IW (2006) Stromatolite reef from the Early Archaean era of Australia. *Nature* **441**, 714–718.
- Altermann W (2004) Evolving life and its effect on Precambrian sedimentation. In *The Precambrian Earth: Times and Events* (eds Eriksson PG, Altermann W, Nelson DR, Mueller W, Catuneanu O). Elsevier, Amsterdam, pp. 539–545.
- Altermann W, Kazmierczak J, Oren A, Wright DT (2006) Cyanobacterial calcification and its rock-building potential during 3.5 billion years of Earth history. *Geobiology* **4**, 147–166.
- Araki S, Eichenberger W, Sakurai T, Sato N (1991) Distribution of diacylglycerylhydroxy-methyltrimethyl-beta-alanine (Dgta) and phosphatidylcholine in brown-algae. *Plant and Cell Physiology* **32**, 623–628.
- Aygun-Sunar S, Mandaci S, Koch HG, Murray IVJ, Goldfine H, Daldal F (2006) Ornithine lipid is required for optimal steady-state amounts of c-type cytochromes in *Rhodobacter capsulatus*. *Molecular Microbiology* **61**, 418–435.
- Baumgartner LK, Reid RP, Dupraz C, Decho AW, Buckley DH, Spear JR, Przekop KM, Visscher PT (2006) Sulfate reducing bacteria in microbial mats: changing paradigms, new discoveries. *Sedimentary Geology* **185**, 131–145.
- Benning C, Huang ZH, Gage DA (1995) Accumulation of a novel glycolipid and a betaine lipid in cells of *Rhodobacter sphaeroides* grown under phosphate limitation. *Archives of Biochemistry and Biophysics* **317**, 103–111.
- Biddle JF, Lipp JS, Lever MA, Lloyd KG, Sorensen KB, Anderson R, Fredricks HF, Elvert M, Kelly TJ, Schrag DP, Sogin ML, Brenchley JE, Teske A, House CH, Hinrichs KU (2006) Heterotrophic archaea dominate sedimentary subsurface ecosystems off Peru. *Proceedings of the National Academy of Sciences of the United States of America* **103**, 3846–3851.
- Blumenberg M, Krüger M, Nauhaus K, Talbot HM, Oppermann BI, Seifert R, Pape T, Michaelis W (2006) Biosynthesis of hopanoids by sulfate-reducing bacteria (genus *Desulfovibrio*). *Environmental Microbiology* **8**, 1220–1227.

- Bosak T, Greene SE, Newman DK (2007) A likely role for anoxygenic photosynthetic microbes in the formation of ancient stromatolites. *Geobiology* **5**, 119–126.
- Boschker HTS, Middelburg JJ (2002) Stable isotopes and biomarkers in microbial ecology. *FEMS Microbiology Ecology* **40**, 85–95.
- Brocks JJ, Summons RE (2003) Sedimentary hydrocarbons, biomarkers for early life. In *Treatise on Geochemistry*, Vol. 8 (eds Holland HD, Turekian KK). Pergamon, Oxford, pp. 63–115.
- Brocks JJ, Logan GA, Buick R, Summons RE (1999) Archean molecular fossils and the early rise of eukaryotes. *Science* **285**, 1033–1036.
- Burns BP, Goh F, Allen M, Neilan BA (2004) Microbial diversity of extant stromatolites in the hypersaline marine environment of Shark Bay, Australia. *Environmental Microbiology* **6**, 1096–1101.
- Campbell S, Golubic S (1985) Benthic cyanophytes (cyanobacteria) of Solar Lake (Sinai). *Archives of Hydrobiology* **38/39**, 311–329.
- Canfield DE, Des Marais DJ (1991) Aerobic sulfate reduction in microbial mats. *Science* **251**, 1471–1473.
- Canfield DE, Sørensen KB, Oren A (2004) Biogeochemistry of a gypsum-encrusted microbial ecosystem. *Geobiology* **2**, 133–150.
- Canfield DE, Kristensen E, Thamdrup B, eds (2005) *Aquatic Geomicrobiology. Advances in Marine Biology*. Elsevier, San Diego, CA.
- Castenholz RW (2001) General characteristics of the cyanobacteria. In *Bergey's Manual of Systematic Bacteriology*, Vol. 1 (eds Boone DR, Castenholz RW). Springer, New York, pp. 474–487.
- Caton TM, Witte LR, Ngyuen HD, Buchheim JA, Buchheim MA, Schneegurt MA (2004) Halotolerant aerobic heterotrophic bacteria from the Great Salt Plains of Oklahoma. *Microbial Ecology* **48**, 449–462.
- Caudales R, Wells JM, Butterfield JE (2000) Cellular fatty acid composition of cyanobacteria assigned to subsection II, order Pleurocapsales. *International Journal of Systematic and Evolutionary Microbiology* **50**, 1029–1034.
- Choma A, Komanićka I (2003) The polar lipid composition of *Mesorhizobium ciceri*. *Biochimica Et Biophysica Acta-Molecular and Cell Biology of Lipids* **1631**, 188–196.
- Chuecas L, Riley JP (1969) Component fatty acids of the total lipids of some marine phytoplankton. *Journal of Marine Biological Association of the UK* **49**, 97–116.
- Cornée A, Dickman M, Busson G (1992) Laminated cyanobacterial mats in sediments of solar salt works – some sedimentological implications. *Sedimentology* **39**, 599–612.
- Craig H (1957) Isotopic standards for carbon and oxygen and correction factors for mass-spectrometric analysis of carbon dioxide. *Geochimica et Cosmochimica Acta* **12**, 133–149.
- Cypionka H, Widdel F, Pfenning N (1985) Survival of sulfate-reducing bacteria after oxygen stress, and growth in sulfate-free oxygen-sulfide gradients. *FEMS Microbiology Ecology* **31**, 39–45.
- Decho AW, Visscher PT, Reid RP (2005) Production and cycling of natural microbial exopolymers (EPS) within a marine stromatolite. *Palaeogeography Palaeoclimatology Palaeoecology* **219**, 71–86.
- Dembitsky VM (1996) Betaine ether-linked glycerolipids: chemistry and biology. *Progress in Lipid Research* **35**, 1–51.
- Dunstan GA, Volkman JK, Barrett SM, Leroi J-M, Jeffrey SW (1994) Essential polyunsaturated fatty acids from 14 species of diatom (Bacillariophyceae). *Phytochemistry* **35**, 155–161.
- Fenchel T (1998a) Formation of laminated cyanobacterial mats in the absence of benthic fauna. *Aquatic Microbial Ecology* **14**, 235–240.
- Fenchel T (1998b) Artificial cyanobacterial mats: cycling of C, O, and S. *Aquatic Microbial Ecology* **14**, 253–259.
- Fischer AG (1965) Fossils, early life and atmospheric history. *Proceedings of the National Academy of Sciences of the United States of America* **53**, 1205–1213.
- Frund C, Cohen Y (1992) Diurnal cycles of sulfate reduction under oxic conditions in cyanobacterial mats. *Applied and Environmental Microbiology* **58**, 70–77.
- García-Pichel F, Nubel U, Muyzer G (1998) The phylogeny of unicellular, extremely halotolerant cyanobacteria. *Archives of Microbiology* **169**, 469–482.
- Geitler L (1932) *Cyanophyceae*. Akademische Verlagsgesellschaft, Leibzig, Germany.
- Ghozlan H, Deif H, Abu Kandil R, Sabry S (2006) Biodiversity of moderately halophilic bacteria in hypersaline habitats in Egypt. *Journal of General and Applied Microbiology* **52**, 63–72.
- Glaeser J, Overmann J (2003) Characterization and *in situ* carbon metabolism of phototrophic consortia. *Applied and Environmental Microbiology* **69**, 3739–3750.
- Grimalt JO, Dewit R, Teixidor P, Albaiges J (1991) Lipid biogeochemistry of Phormidium and Microcoleus mats. *Organic Geochemistry* **19**, 509–530.
- Gugger M, Lyra C, Suominen I, Tsitko I, Humbert JF, Salkinoja-Salonen MS, Sivonen K (2002) Cellular fatty acids as chemotaxonomic markers of the genera Anabaena, Aphanizomenon, Microcystis, Nostoc and Planktothrix (cyanobacteria). *International Journal of Systematic and Evolutionary Microbiology* **52**, 1007–1015.
- Hanford M, Peebles TL (2002) Archaeal tetraether lipids – unique structures and applications. *Applied Biochemistry and Biotechnology* **97**, 45–62.
- Härtner T, Straub KL, Kanning E (2005) Occurrence of hopanoid lipids in anaerobic *Geobacter* species. *FEMS Microbiology Letters* **243**, 59–64.
- Hayes JM (2001) Fractionation of carbon and hydrogen isotopes in biosynthetic processes. *Reviews in Mineralogy & Geochemistry* **43**, 225–277.
- Hirschler-Rea A, Matheron R, Riffaud C, Moune S, Eatock C, Herbert RA, Willison JC, Caumette P (2003) Isolation and characterization of spirilloid purple phototrophic bacteria forming red layers in microbial mats of Mediterranean salterns: description of *Halorhodospira neutriphila* sp nov and emendation of the genus *Halorhodospira*. *International Journal of Systematic and Evolutionary Microbiology* **53**, 153–163.
- Hoehler TM, Bebout BM, Des Marais DJ (2001) The role of microbial mats in the production of reduced gases on the early Earth. *Nature* **412**, 324–327.
- Holland HD (2006) The oxygenation of the atmosphere and oceans. *Philosophical Transactions of the Royal Society B-Biological Sciences* **361**, 903–915.
- Hopmans EC, Schouten S, Pancost RD, van der Meer MTJ, Damste JSS (2000) Analysis of intact tetraether lipids in archaeal cell material and sediments by high performance liquid chromatography/atmospheric pressure chemical ionization mass spectrometry. *Rapid Communications in Mass Spectrometry* **14**, 585–589.
- Imhoff JF, Kushner DJ, Kushwaha SC, Kates M (1982) Polar lipids in phototropic bacteria of the rhodospirillaceae and chromatiaaceae families. *Journal of Bacteriology* **150**, 1192–1201.
- Jahnke LL, Eder W, Huber R, Hope JM, Hinrichs KU, Hayes JM, Des Marais DJ, Cady SL, Summons RE (2001) Signature lipids and stable carbon isotope analyses of octopus spring hyperthermophilic communities compared with those of

- Aquificales representatives. *Applied and Environmental Microbiology* **67**, 5179–5189.
- Jahnke LL, Orphan VJ, Embaye T, Turk KA, Kubo MD, Summons RE, Des Marais DJ (2008) Lipid biomarker and phylogenetic analyses to reveal archaeal biodiversity and distribution in hypersaline microbial mat and underlying sediment. *Geobiology* **6**, 394–410.
- Javor BJ (2002) Industrial microbiology of solar salt production. *Journal of Industrial Microbiology & Biotechnology* **28**, 42–47.
- Jonkers HM, Ludwig R, De Wit R, Pringault O, Muyzer G, Niemann H, Finke N, De Beer D (2003) Structural and functional analysis of a microbial mat ecosystem from a unique permanent hypersaline inland lake: 'La Salada de Chiprana' (NE Spain). *FEMS Microbiology Ecology* **44**, 175–189.
- Jørgensen BB, Revsbech NP, Cohen Y (1983) Photosynthesis and structure of benthic microbial mats – microelectrode and SEM studies of 4 cyanobacterial communities. *Limnology and Oceanography* **28**, 1075–1093.
- Joyeux C, Fouchard S, Llopiz P, Neunlist S (2004) Influence of the temperature and the growth phase on the hopanoids and fatty acids content of *Frateruia aurantia* (DSMZ 6220). *FEMS Microbiology Ecology* **47**, 371–379.
- Kenyon CN, Stanier RY, Rippka R (1972) Fatty-acid composition and physiological properties of some filamentous blue-green algae. *Archiv für Mikrobiologie* **83**, 216–236.
- King GM (1988) Methanogenesis from methylated amines in a hypersaline algal mat. *Applied and Environmental Microbiology* **54**, 130–136.
- Kiseleva LL, Horvath I, Vigh L, Los DA (1999) Temperature-induced specific lipid desaturation in the thermophilic cyanobacterium *Synechococcus vulcanus*. *FEMS Microbiology Letters* **175**, 179–183.
- Knoll AH (2003) The geological consequences of evolution. *Geobiology* **1**, 3–14.
- Knoll AH, Summons RE, Waldbauer JR, Zumberge J (2007) The geological succession of primary producers in the oceans. In *The Evolution of Primary Producers in the Sea* (eds Falkowski P, Knoll AH). Academic Press, Boston, MA, pp. 133–163.
- Koga Y, Morii H, Akagawa-Matsushita M, Ohga I (1998) Correlation of polar lipid composition with 16S rRNA phylogeny in methanogens. Further analysis of lipid component parts. *Bioscience Biotechnology and Biochemistry* **62**, 230–236.
- Komárek J, Anagnostidis K (1999) *Cyanoprokaryota, 1. Teil: Chroococcales*. Gustav Fischer Verlag, Jena, Germany.
- Komárek J, Anagnostidis K (2005) *Cyanoprokaryota, 2. Teil: Oscillatoriales*. Gustav Fischer Verlag, Jena, Germany.
- Krekeler D, Teske A, Cypionka H (1998) Strategies of sulfate-reducing bacteria to escape oxygen stress in a cyanobacterial mat. *FEMS Microbiology Ecology* **25**, 89–96.
- Lechevalier H, Lechevalier MP (1988) Chemotaxonomic use of lipids – an overview. *Microbial lipids* (eds Ratledge C, Wilkinson SG). Academic Press, London, pp. 869–902.
- Linscheid M, Diehl BWK, Overmohle M, Riedl I, Heinz E (1997) Membrane lipids of *Rhodospseudomonas viridis*. *Biochimica Et Biophysica Acta-Lipids and Lipid Metabolism* **1347**, 151–163.
- Lipp JS, Morono Y, Inagaki F, Hinrichs K-U (2008) Significant contribution of Archaea to extant biomass in marine subsurface sediments. *Nature* **454**, 991–994.
- Lochte K, Turley CM (1988) Bacteria and cyanobacteria associated with phytodetritus in the deep sea. *Nature* **333**, 67–69.
- Londry KL, Dawson KG, Grover HD, Summons RE, Bradley AS (2008) Stable carbon isotope fractionation between substrates and products of *Methanosarcina barkeri*. *Organic Geochemistry* **2008**, 608–621.
- Lopez-Lara IM, Sohlenkamp C, Geiger O (2003) Membrane lipids in plant-associated bacteria: their biosyntheses and possible functions. *Molecular Plant-Microbe Interactions* **16**, 567–579.
- Manske AK, Glaeser J, Kuypers MMM, Overmann J (2005) Physiology and phylogeny of green sulfur bacteria forming a monospecific phototrophic assemblage at a depth of 100 meters in the Black Sea. *Applied and Environmental Microbiology* **71**, 8049–8060.
- van der Meer MTJ, Schouten S, Sinninghe Damste JS, Ward DM (2007) Impact of carbon metabolism on C-13 signatures of cyanobacteria and green non-sulfur-like bacteria inhabiting a microbial mat from an alkaline siliceous hot spring in Yellowstone National Park (USA). *Environmental Microbiology* **9**, 482–491.
- Middelburg JJ, Barranguet C, Boschker HTS, Herman PMJ, Moens T, Heip CHR (2000) The fate of intertidal microphytobenthos: an *in situ* ¹³C labelling study. *Limnology and Oceanography* **45**, 1224–1234.
- Mir J, Martinezalonso M, Esteve I, Guerrero R (1991) Vertical stratification and microbial assemblage of a microbial mat in the Ebro Delta (Spain). *FEMS Microbiology Ecology* **86**, 59–68.
- Nübel U, Bateson MM, Vandieken V, Wieland A, Kühl M, Ward DM (2002) Microscopic examination of distribution and phenotypic properties of phylogenetically diverse Chloroflexaceae-related bacteria in hot spring microbial mats. *Applied and Environmental Microbiology* **68**, 4593–4603.
- Okazaki K, Sato N, Tsuji N, Tsuzuki M, Nishida I (2006) The significance of C16 fatty acids in the sn-2 positions of glycerolipids in the photosynthetic growth of *Synechocystis* sp PCC6803. *Plant Physiology* **141**, 546–556.
- Orphan VJ, Jahnke LL, Embaye T, Turk KA, Pernthaler A, Summons RE, Des Marais DJ (2008) Characterization and spatial distribution of methanogens and methanogenic biosignatures in hypersaline microbial mats of Baja California. *Geobiology* **6**, 376–393.
- de Oteyza TG, Lopez JF, Grimalt JO (2004) Fatty acids, hydrocarbons, sterols and alkenones of microbial mats from coastal ecosystems of the Ebro Delta. *Ophelia* **58**, 189–194.
- Ourisson G, Rohmer M, Poralla K (1987) Prokaryotic hopanoids and other polyterpenoid sterol surrogates. *Annual Review of Microbiology* **41**, 301–333.
- Papineau D, Walker JJ, Mojzsis SJ, Pace NR (2005) Composition and structure of microbial communities from stromatolites of Hamelin Pool in Shark Bay, Western Australia. *Applied and Environmental Microbiology* **71**, 4822–4832.
- Permentier HP, Neerken S, Schmidt KA, Overmann J, Amez J (2000) Energy transfer and charge separation in the purple non-sulfur bacterium *Roseospirillum parvum*. *Biochimica Et Biophysica Acta-Bioenergetics* **1460**, 338–345.
- Peterson BJ (1999) Stable isotopes as tracers of organic matter input and transfer in benthic food webs: a review. *Acta Oecologica* **20**, 479–487.
- Pinckney JL, Paerl HW (1997) Anoxygenic photosynthesis and nitrogen fixation by a microbial mat community in a Bahamian hypersaline lagoon. *Applied and Environmental Microbiology* **63**, 420–426.
- Postgate JR (1959) Sulphate reduction by bacteria. *Annual Review of Microbiology* **13**, 505–520.
- Potts M (1994) Desiccation tolerance of prokaryotes. *Microbiological Reviews* **58**, 755–805.
- Rajendran N, Matsuda O, Imamura N, Urushigawa Y (1992) Variation in microbial biomass and community structure in sediments of eutrophic bays as determined by phospholipid

- ester-linked fatty acid. *Applied and Environmental Microbiology* **58**, 562–571.
- Ratledge C, Wilkinson SG (1988) *Microbial Lipids*. Academic Press, London.
- Richert L, Golubic S, Le Guedes R, Herve A, Payri C (2006) Cyanobacterial populations that build 'kopara' microbial mats in Rangiroa, Tuamotu Archipelago, French Polynesia. *European Journal of Phycology* **41**, 259–279.
- Ritter D, Yopp JH (1993) Plasma-membrane lipid-composition of the halophilic cyanobacterium *Aphanothece halophytica*. *Archives of Microbiology* **159**, 435–439.
- Rohmer M, Bouviernave P, Ourisson G (1984) Distribution of Hopanoid Triterpenes in Prokaryotes. *Journal of General Microbiology* **130**, 1137–1150.
- Romano I, Finore I, Nicolaus G, Huertas FJ, Lama L, Nicolaus B, Poli A (2008) *Halobacillus alkaliphilus* sp nov., a halophilic bacterium isolated from a salt lake in Fuente de Piedra, southern Spain. *International Journal of Systematic and Evolutionary Microbiology* **58**, 886–890.
- Rosa-Putra S, Nalin R, Domenach AM, Rohmer M (2001) Novel hopanoids from Frankia spp. and related soil bacteria – Squalene cyclization and significance of geological biomarkers revisited. *European Journal of Biochemistry* **268**, 4300–4306.
- Rütters H, Sass H, Cypionka H, Rullkötter J (2002a) Phospholipid analysis as a tool to study complex microbial communities in marine sediments. *Journal of Microbiological Methods* **48**, 149–160.
- Rütters H, Sass H, Cypionka H, Rullkötter J (2002b) Microbial communities in a Wadden Sea sediment core – clues from analyses of intact glyceride lipids, and released fatty acids. *Organic Geochemistry* **33**, 803–826.
- Sachse D, Sachs JP (2008) Inverse relationship between D/H fractionation in cyanobacterial lipids and salinity in Christmas Island saline ponds. *Geochimica et Cosmochimica Acta*, **73**, 793–806.
- Saenger C, Miller M, Smittenberg RH, Sachs JP (2006) A physico-chemical survey of inland lakes and saline ponds: Christmas Island (Kirimati) and Washington (Teraina) Island, Republic of Kiribati. *Saline Systems* **2**, 8.
- Schidlowski M, Hayes JM, Kaplan IR (1983) Isotopic inferences of ancient biogeochemistries: carbon, sulfur, hydrogen, and nitrogen. In *Earth's Earliest Biosphere: Its Origin and Evolution* (eds Schopf W). Princeton University Press, Princeton, NJ, pp. 149–187.
- Schopf JW (2006) Fossil evidence of Archaean life. *Philosophical Transactions of the Royal Society B-Biological Sciences* **361**, 869–885.
- Schubotz F (2005) *Investigation of Intact Polar Lipids of Bacteria Isolated from Deep Marine Subsurface*. MSc Thesis. University of Bremen, Bremen, Germany, 95 pp.
- Sinninghe Damste JS, Rijpstra WIC, Hopmans EC, Prahl FG, Wakeham SG, Schouten S (2002) Distribution of membrane lipids of planktonic Crenarchaeota in the Arabian sea. *Applied and Environmental Microbiology* **68**, 2997–3002.
- Sørensen KB, Canfield DE, Teske AP, Oren A (2005) Community composition of a hypersaline endoevaporitic microbial mat. *Applied and Environmental Microbiology* **71**, 7352–7365.
- Sturt HF, Summons RE, Smith K, Elvert M, Hinrichs KU (2004) Intact polar membrane lipids in prokaryotes and sediments deciphered by high-performance liquid chromatography/electrospray ionization multistage mass spectrometry – new biomarkers for biogeochemistry and microbial ecology. *Rapid Communications in Mass Spectrometry* **18**, 617–628.
- Summons RE, Jahnke LL, Roksanid Z (1994) Carbon isotopic fractionation in lipids from methanotrophic bacteria: relevance for interpretation of the geochemical record of biomarkers. *Geochimica et Cosmochimica Acta* **58**, 2853–2863.
- Summons RE, Jahnke LL, Simoneit BRT (1996) Lipid biomarkers for bacterial ecosystems: studies of cultured organisms, hydrothermal environments and ancient sediments. In *Evolution of Hydrothermal Ecosystems on Earth (and Mars?)* (eds Bock G, Goode J), CIBA Foundation Symposium 202. Wiley, Chichester, pp. 174–194.
- Summons RE, Franzmann PD, Nichols PD (1998) Carbon isotopic fractionation associated with methylophilic methanogenesis. *Organic Geochemistry* **28**, 465–475.
- Summons RE, Jahnke LL, Hope JM, Logan GA (1999) 2-Methylhopanoids as biomarkers for cyanobacterial oxygenic photosynthesis. *Nature* **400**, 554–557.
- Takahashi Y, Matsumoto E, Watanabe YW (2000) The distribution of delta C-13 in total dissolved inorganic carbon in the central North Pacific Ocean along 175 degrees E and implications for anthropogenic CO2 penetration. *Marine Chemistry* **69**, 237–251.
- Talbot HM, Farrimond P (2007) Bacterial populations recorded in diverse sedimentary biohopanoid distributions. *Organic Geochemistry* **38**, 1212–1225.
- Talbot HM, Summons RE, Jahnke LL, Cockell CS, Rohmer M, Farrimond P (2008) Cyanobacterial bacteriohopanepolyol signatures from cultures and natural environmental settings. *Organic Geochemistry* **39**, 232–263.
- Valencia MJ (1977) Christmas Island (Pacific Ocean): reconnaissance geologic observations. *Atoll Research Bulletin* **197**, 1–17.
- Van Mooy BAS, Rocap G, Fredricks HF, Evans CT, Devol AH (2006) Sulfolipids dramatically decrease phosphorus demand by picocyanobacteria in oligotrophic marine environments. *Proceedings of the National Academy of Sciences of the United States of America* **103**, 8607–8612.
- Volkman JK (1986) A review of sterol markers for marine and terrigenous organic-matter. *Organic Geochemistry* **9**, 83–99.
- Volkman JK, Maxwell JR (1986) Acyclic isoprenoids as biological markers. In *Biological Markers in the Sedimentary Record* (eds Johns RB). Elsevier, New York, pp. 1–42.
- Wada H, Murata N (1998) Membrane lipids in cyanobacteria. In *Lipids in Photosynthesis: Structure, Function and Genetics* (eds Siegenthaler PA, Murata N). Kluwer Academic Publishers, Dordrecht, pp. 65–81.
- Weissenmayer B, Gao JL, Lopez-Lara IM, Geiger O (2002) Identification of a gene required for the biosynthesis of ornithine-derived lipids. *Molecular Microbiology* **45**, 721–733.
- Wieland A, Kühl M, McGowan L, Fourcans A, Duran R, Caumette P, de Oteyza TG, Grimalt JO, Sole A, Diestra E, Esteve I, Herbert RA (2003) Microbial mats on the Orkney Islands revisited: microenvironment and microbial community composition. *Microbial Ecology* **46**, 371–390.
- Woodroffe CD, McLean RF (1998) Pleistocene morphology and Holocene emergence of Christmas (Kiritimati) Island, Pacific Ocean. *Coral Reefs* **17**, 235–248.